European Journal of Neuroscience, Vol. 18, pp. 1775–1785, 2003 *© Federation of European Neuroscience Societies*

Hypocretin-1 causes G protein activation and increases ACh release in rat pons

René Bernard,[1] Ralph Lydic[2] and Helen A. Baghdoyan[1,2]
Departments of [1]Pharmacology and
[2]Anaesthesiology, University of Michigan, 7433 Medical Sciences Building I, 1150 West Medical Center Drive, Ann Arbor, MI 48109, USA

Keywords: [^{35}S]GTPγS autoradiography, dorsal raphe nucleus, locus coeruleus, orexin, REM sleep

Abstract

The effects of the arousal-promoting peptide hypocretin on brain stem G protein activation and ACh release were examined using 16 adult Sprague-Dawley rats. *In vitro* [^{35}S]GTPγS autoradiography was used to test the hypothesis that hypocretin-1-stimulated G protein activation is concentration-dependent and blocked by the hypocretin receptor antagonist SB-334867. Activated G proteins were quantified in dorsal raphe nucleus (DR), locus coeruleus (LC) and pontine reticular nucleus oral part (PnO) and caudal part (PnC). Concentration–response data revealed a significant ($P < 0.001$) effect of hypocretin-1 (2–2000 nM) in all brain regions examined. Maximal increases over control levels of [^{35}S]GTPγS binding were 37% (DR), 58% (LC), 52% (PnO) and 44% (PnC). SB-334867 (2 μM) significantly ($P < 0.002$) blocked hypocretin-1 (200 nM)-stimulated [^{35}S]GTPγS binding in all four nuclei. This is the first autoradiographic demonstration that hypocretin-1 activates G proteins in arousal-related brain stem nuclei as a result of specific receptor interactions. This finding suggests that some hypocretin receptors in brain stem couple to inhibitory G proteins. *In vivo* microdialysis was used to test the hypothesis that PnO administration of hypocretin-1 increases ACh release in PnO. Dialysis delivery of hypocretin-1 (100 μM) significantly ($P < 0.002$) increased (87%) ACh release. This finding is consistent with the interpretation that one mechanism by which hypocretin promotes arousal is by enhancing cholinergic neurotransmission in the pontine reticular formation.

Introduction

The hypothalamic neuropeptides hypocretin (hcrt)-1 and hcrt-2 (de Lecea *et al*., 1998), also named orexin-A and orexin-B (Sakurai *et al*., 1998), are thought to participate in the regulation of behavioural arousal (Kilduff & Peyron, 2000). In animals, intracranial administration of hcrt increases wakefulness (Hagan *et al*., 1999; Bourgin *et al*., 2000; Piper *et al*., 2000; España *et al*., 2001; Xi *et al*., 2001), and experimentally induced losses of hcrt neurons disrupt wakefulness (Gerashchenko *et al*., 2001; Hara *et al*., 2001). Animal models of the human sleep disorder narcolepsy are characterized by defective hcrt receptors (Lin *et al*., 1999) or a lack of the peptide (Chemelli *et al*., 1999), and human narcoleptic patients show low or undetectable hcrt levels in cerebrospinal fluid (Nishino *et al*., 2000, 2001) and a loss of hcrt neurons (Peyron *et al*., 2000; Thannickal *et al*., 2000). The clinical phenotype of narcolepsy includes excessive daytime sleepiness, disrupted nighttime sleep and the onset of rapid eye movement (REM) sleep periods or traits directly from wakefulness (Nishino & Mignot, 1997). Narcolepsy can be viewed as a disorder of the normal boundaries between different arousal states, and it has been suggested that the loss of hypocretin in narcolepsy may facilitate inappropriate transitions between wakefulness and sleep (Scammell, 2003).

The mechanisms by which hcrt regulates states of arousal are not well understood. Hcrt-synthesizing neurons project to arousal-promoting brain stem nuclei including the dorsal raphe nucleus (DR), locus coeruleus (LC) and pontine reticular nucleus, oral part (PnO) and caudal part (PnC) (Peyron *et al*., 1998). Hcrt excites noradrenergic LC (Hagan *et al*., 1999; Horvath *et al*., 1999) and serotonergic DR (Brown *et al*., 2001) neurons, and may promote wakefulness by elevating monoaminergic tone (Kilduff & Peyron, 2000). Hcrt-1 microinjection into cat pontine reticular formation triggers REM sleep (Xi *et al*., 2002), suggesting that hcrt-1 may also promote brain activation by enhancing pontine cholinergic neurotransmission (Kilduff & Peyron, 2000).

Hcrt binds two guanine nucleotide binding protein (G protein)-coupled receptors, hcrt-r1 and hcrt-r2 (Sakurai *et al*., 1998). Hcrt-r1 shows a higher affinity for hcrt-1 than for hcrt-2, whereas hcrt-r2 shows equally high affinity for both peptides (Sakurai *et al*., 1998). *In vitro* [^{35}S]guanylyl-5′-O-(γ-thio)triphosphate ([^{35}S]GTPγS) autoradiography offers a unique approach for identifying brain regions where agonists bind to receptors to cause G protein activation (Sim *et al*., 1995; Sóvágó *et al*., 2001). Hcrt-1 has been shown to activate G proteins in arousal-related brain stem nuclei (Bernard *et al*., 2002a). The present study used *in vitro* [^{35}S]GTPγS autoradiography to test the hypothesis that hcrt-1-stimulated G protein activation in DR, LC, PnO and PnC is concentration-dependent, saturates, and can be blocked by the hcrt receptor antagonist SB-334867 (Smart *et al*., 2001). The hypothesis was confirmed, indicating that hcrt-induced [^{35}S]GTPγS binding is receptor-mediated. An *in vivo* consequence of hcrt-1-stimulated G protein activation was investigated by testing the additional hypothesis that microdialysis delivery of hcrt-1 to rat PnO increases ACh release in PnO. The second hypothesis was supported, consistent with the interpretation that one mechanism by which hcrt produces arousal may be by enhancing pontine cholinergic neurotransmission. Portions of these data have been presented as abstracts (Bernard *et al*., 2002b; Bernard *et al*., 2003a).

Correspondence: Helen A. Baghdoyan, as above.
E-mail: helenb@umich.edu

Received 25 March 2003, revised 17 July 2003, accepted 22 July 2003

doi:10.1046/j.1460-9568.2003.02905.x

Materials and methods

Chemicals and animals

Hcrt-1 was purchased from California Peptide Research (Napa, CA, USA). SB-334867 was provided by GlaxoSmithKline (Essex, UK). Reflection autoradiography film (Kodak X-OMAT Blue XB-1) and [^{35}S]GTPγS were obtained from PerkinElmer Life Science Products (Boston, MA, USA). Carbachol, guanosine 5′-diphosphate (GDP), guanosine 5′-O-(γ-thio)triphosphate (GTPγS), and chemicals used for buffers, Ringer's solution, standard curves and mobile phase were purchased from Sigma-Aldrich (St Louis, MO, USA). Adult male Sprague-Dawley rats (250–350 g) were purchased from Charles River Laboratories (Wilmington, MA, USA) and housed in a 12-h light–dark cycle for at least 1 week prior to use. All experiments were performed in accordance with the Guide for the Care and Use of Laboratory Animals (National Academy Press, Washington, DC, 1996) and with approval by the University of Michigan Committee on Use and Care of Animals.

Preparing tissue sections and performing in vitro *[^{35}S]GTPγS autoradiography*

Rats were always decapitated at the same time of day (4–5 h after light onset). Brains were removed and immediately frozen in a bilayer composed of 2-methylbutane and 1-bromobutane at −30 °C. Coronal brain stem sections (20 μm thick) were cut serially using Hacker Bright (Fairfield, NJ, USA) or Leica CM3050 S (Leica Microsystems, Nussloch, Germany) cryostats. Adjacent pairs of sections from approximately bregma −10.30 to −7.04 mm (Paxinos & Watson, 1998) were thaw-mounted onto gelatin-coated glass slides, dried in a vacuum desiccator (4 °C) and stored at −70 °C before being used in an assay.

[^{35}S]GTPγS binding assays were performed as previously described (Sim *et al*., 1995; Capece *et al*., 1998; Bernard *et al*., 2002a). Assay buffer contained 50 mM Tris-HCl, 3 mM MgCl, 0.2 mM EGTA and 100 mM NaCl (pH 7.4). Slide-mounted tissue sections were brought to room temperature and incubated for 2 h in 0.04 nM [^{35}S]GTPγS and 2 mM GDP. Different drug treatments during the 2-h incubation were applied for the concentration–response assays and for the antagonist blocking assays, as described below. For all assays, the incubation period was terminated by rinsing tissue sections in ice-cold 50 mM Tris-HCl buffer (pH 7.0) followed by ice-cold deionized water.

For the concentration–response assays, tissue sections were assigned serially to one of seven assay conditions. The first assay condition determined basal [^{35}S]GTPγS binding in the absence of an exogenous agonist. Conditions two to five contained hcrt-1 (2, 20, 200 or 2000 nM, respectively) to test the hypothesis that hcrt-1-stimulated G protein activation is concentration-dependent. Condition six used the cholinergic agonist carbachol (1 mM) as a positive assay control (Capece *et al*., 1998). Assay condition seven determined nonspecific binding using excess unlabelled GTPγS (10 μM).

For the study designed to test the hypothesis that hcrt-1-stimulated G protein activation can be blocked by the specific hcrt receptor antagonist SB-334867, tissue sections were assigned serially to one of five assay conditions: basal, nonspecific binding, hcrt-1 (200 nM), SB-334867 (2 μM), and hcrt-1 (200 nM) + SB-334867 (2 μM). SB-334867 is poorly soluble in water, requiring the use of dimethyl sulfoxide (DMSO) (Duxon *et al*., 2001). To control for nonspecific effects of DMSO on [^{35}S]GTPγS binding, the buffer used for all five assay conditions contained 0.02% DMSO.

Post-assay processing of the tissue sections included drying, exposing to autoradiography film, and staining. Tissue sections were initially dried in a room-temperature stream of air. The drying process was completed by keeping the sections in a vacuum desiccator overnight. The sections were then put into autoradiography cassettes (Fisher Scientific, Pittsburg, PA, USA) together with ^{14}C microscale standards (31–883 nCi/g, Amersham Biosciences, Arlington Heights, IL, USA) and X-OMAT Blue XB-1 film (Eastman Kodak Company, Rochester, NY, USA). After 72 h of exposure at room temperature, films were developed with a Kodak X-OMAT Model 2002A film processor. Tissue sections were fixed with paraformaldehyde vapors (80 °C) and stained with Cresyl Violet.

Quantifying [^{35}S]GTPγS binding

A Cohu CCD camera with a Micro Nikon 60 mm objective, the Scion Image 1.62c version of NIH Image, and a G3 Apple Macintosh computer were used to produce digital images from each autoradiogram and Cresyl Violet-stained tissue section. The following procedure was used to quantify [^{35}S]GTPγS binding in DR, LC, PnO, and PnC. Each nucleus was localized and digitally outlined on the Cresyl Violet image according to a rat brain atlas (Paxinos & Watson, 1998). Outlines were transferred to the identical position on the digitized version of the autoradiogram and optical density was quantified. To calculate total [^{35}S]GTPγS binding, optical density was converted to nCi/g brain tissue using a ^{14}C correction factor (Capece *et al*., 1998). Mean nonspecific binding values for each of the four nuclei were subtracted from individual total [^{35}S]GTPγS binding values to produce specific binding values for each nucleus. The number of individual optical density measurements obtained from each nucleus is dependent on the rostral-to-caudal extent of that nucleus and whether the nucleus is a midline (DR) or a bilateral (LC, PnO, PnC) structure. An average specific binding value was calculated for each nucleus from every animal.

Data were analysed using one-way analysis of variance (ANOVA) and Tukey–Kramer multiple comparisons test. The alpha level was set at $P < 0.05$. GraphPad Prism software (version 3.0a for Macintosh, GraphPad Software, San Diego, CA, USA) was used for nonlinear regression analysis of hcrt-1 concentration–response binding data. Sigmoid curves were fitted using the following equation:

$$\text{specific } [^{35}\text{S}]GTP\gamma\text{S binding} = \text{basal binding} + (\text{maximal binding} - \text{basal binding})/(1+10\hat{}(\log \text{EC}_{50} - X))$$

where X represents the logarithm of the hcrt-1 concentration. These analyses were used to determine the concentration of hcrt-1 which produced 50% of the maximal increase in [^{35}S]GTPγS binding (EC_{50}) and the coefficient of determination (r^2) for each nucleus.

Measuring the effects of hcrt-1 on pontine ACh release

Every microdialysis experiment was performed according to the following series of procedures. After quantifying the percentage of ACh recovered *in vitro* by a dialysis probe, a rat was anaesthetized and the probe was aimed stereotaxically for either the left or right PnO; details are given below. *In vivo* dialysis samples were collected and immediately analysed for ACh content. The dialysis probe was removed from the brain and probe recovery of ACh again was determined *in vitro*. Each rat was used for only one experiment. Placement of the dialysis probe in the PnO was confirmed histologically. These steps are described in detail below.

Using in vivo microdialysis to deliver hcrt-1 to the pons and collect ACh from the pons

CMA/11 microdialysis probes (1 mm length, 0.24 mm membrane diameter, 6 kDa cut-off; CMA Microdialysis, North Chelmsford, MA, USA) were connected to a CMA/100 pump which provided a constant 2.0 μL/min flow rate. Probes were perfused continuously with either Ringer's solution (147 mM NaCl, 4.0 mM KCl, 2.4 mM $CaCl_2$,

10 μM neostigmine bromide, pH 5.8–6.2) or with hcrt-1 (100 μM) dissolved in Ringer's solution and adjusted to pH 5.8–6.2 with NaOH. Dialysis samples (30 μL) were collected every 15 min. Before positioning the dialysis probe in the brain, the probe was placed in a solution of known ACh concentration and five 30-μL samples were collected and analysed for ACh. These data were used to calculate percentage of ACh recovered by the probe.

Rats were deeply anaesthetized with 3–4% isoflurane (Abbott Laboratories, North Chicago, IL, USA) in 100% O_2 and placed in a Model 962 ultra-precise small-animal stereotaxic instrument (David Kopf Instruments, Tujunga, CA, USA) equipped with a Model 920 rat adaptor, anaesthesia mask and ear bars. A warm water blanket (37 °C) connected to a re-circulating heat pump system (Gaymar Industries, Orchard Park, NY, USA) was used to maintain body temperature during anaesthesia. Delivered isoflurane concentration and core body temperature were measured using a Cardiocap™/5 monitor (Datex-Ohmeda, Madison, WI, USA). Respiratory rate (breaths/min) was counted manually every 15 min. The scalp was opened and an access hole for the dialysis probe was made through the skull using a Dremel (Racine, WI, USA). A dialysis probe was aimed for the PnO according to the following stereotaxic coordinates: 8.6 mm posterior to bregma, 1.2 mm lateral from the midline and 9.2 mm ventral to bregma (Paxinos & Watson, 1998).

After the dialysis probe was in the brain, delivered isoflurane concentration was set at 1.5% and held constant during sample collection. Dialysis samples were collected for at least 45 min to ensure stable ACh levels. Five control samples (75 min) then were collected during dialysis with Ringer's solution before hcrt-1 delivery was initiated by turning a CMA/110 liquid switch. Five dialysis samples (75 min) were collected during hcrt-1 delivery. When the dialysis probe was removed from the brain, the scalp wound was closed using sutures. Animals were allowed to recover from anaesthesia and survive 3–4 days to permit formation of a glial scar at the site where the dialysis probe had been placed.

Immediately following removal of the dialysis probe from the brain, the probe was placed in a solution of known ACh concentration and five dialysis samples were collected and analysed for ACh. Comparison between pre- and postexperimental probe recoveries by two-sample Student's *t*-test ($P < 0.05$) ensured that changes in ACh release measured during each experiment resulted from drug administration and not from intraexperimental changes in the dialysis membrane (Vazquez & Baghdoyan, 2003). The present study includes only experiments where pre- and postexperimental probe recoveries did not change significantly in the hypothesized direction of the drug effect.

Quantifying ACh

Dialysis samples were analysed by high performance liquid chromatography with electrochemical detection (Bioanalytical Systems (BAS), West Lafayette, IN, USA, as previously described (Baghdoyan *et al*., 1998; Vazquez & Baghdoyan, 2003). ACh was converted proportionally into H_2O_2 by an immobilized enzyme reactor column and H_2O_2 was detected amperometrically by a platinum electrode (+0.5 V) in reference to a Ag^+/AgCl electrode. The subsequent chromatographic signal was digitized and quantified using ChromGraph® software (BAS) and a five-point standard curve (0.1–1.0 pmol ACh) created before each experiment. Differences in ACh before and during hcrt-1 administration were evaluated using paired *t*-test. The alpha level for statistical significance was $P < 0.05$.

Histologically identifying dialysis probe sites

Rats were killed with an overdose of anaesthetic, and brains were removed for verification of probe placement. Brains were frozen immediately after removal and cut serially as 40-μm coronal sections using a Leica cryostat. Sections then were fixed using paraformaldehyde vapors (80 °C), stained with Cresyl Violet, and visually inspected for evidence of a dialysis probe-induced lesion. Every section containing a lesion was digitized using a Cohu CCD camera with a Micro Nikon 60-mm objective. Digitized sections were compared with coronal plates from a rat brain atlas (Paxinos & Watson, 1998) to determine the stereotaxic coordinates for each dialysis site.

Results

Hcrt-1-induced G protein activation was concentration-dependent and blocked by the hcrt receptor antagonist SB-334867

Figure 1 illustrates G protein activation by hcrt-1 in the pontine brain stem. Colour-coded autoradiograms show total [^{35}S]GTPγS binding under basal conditions and after *in vitro* treatment with hcrt-1 (2000 nM). Increased [^{35}S]GTPγS binding over basal levels is indicated by more green, yellow and red colours. The boundaries of pontine brain stem nuclei where [^{35}S]GTPγS binding was quantified and found to be significantly increased by hcrt-1 are outlined. These four nuclei include LC, PnC, DR and PnO. Visual inspection reveals that hcrt-1 also increased [^{35}S]GTPγS binding in the posterodorsal tegmental nucleus (PDTg), ventrolateral periaqueductal grey (VLPAG) and median raphe nucleus (MnR). No [^{35}S]GTPγS binding was observed in the facial nerve (7n).

Figure 2 summarizes basal and hcrt-1-stimulated specific [^{35}S]GTPγS binding quantified for DR, LC, PnC and PnO. Results are based on 744 individual measurements obtained from four brains for DR, LC and PnC, and three brains for PnO. ANOVA revealed a significant concentration main effect of hcrt-1 on G protein activation in DR (Fig. 2A; $F_{4,19} = 27.6$, $P < 0.0001$), LC (Fig. 2B; $F_{4,19} = 11.4$, $P = 0.0005$), PnC (Fig. 2C; $F_{4,19} = 21.5$, $P < 0.0001$) and PnO (Fig. 2D; $F_{4,14} = 33.4$, $P < 0.0001$). For all four nuclei, Tukey–Kramer multiple comparisons tests showed that [^{35}S]GTPγS binding induced by 20, 200 and 2000 nM hcrt-1 was significantly increased over basal levels. Hcrt-1 maximally increased [^{35}S]GTPγS binding over basal values by 37% in DR (Fig. 2A), 58% in LC (Fig. 2B), 44% in PnC (Fig. 2C) and 52% in PnO (Fig. 2D).

Figure 3 provides quantitative data illustrating pharmacological antagonism of hcrt-1-stimulated [^{35}S]GTPγS binding by SB-334867. Results consist of 1496 measurements taken from six brains for DR, PnC and PnO, and five brains for LC. Repeated-measures ANOVA and *post hoc* Tukey–Kramer multiple comparisons tests showed that treatment with SB-334867 significantly decreased specific [^{35}S]GTPγS binding induced by 200 nM hcrt-1 in DR (Fig. 3A; $F_{3,23} = 20.0$, $P < 0.0001$), LC (Fig. 3B; $F_{3,19} = 8.9$, $P = 0.002$), PnC (Fig. 3C; $F_{3,23} = 22.6$, $P < 0.0001$) and PnO (Fig. 3D; $F_{3,23} = 24.7$, $P < 0.0001$). SB-334867 did not alter [^{35}S]GTPγS binding in any nucleus studied.

Microdialysis delivery of hcrt-1 increased ACh release in the pontine reticular formation

The demonstration that *in vitro* treatment with hcrt-1 caused a concentration-dependent activation of G proteins in arousal-related nuclei encourages investigations into the functional consequences of *in vivo* hcrt-1 administration. Therefore, this study used dialysis to deliver hcrt-1 to the PnO while measuring ACh release in the PnO. Figure 4 summarizes histological data confirming that all dialysis sites were restricted to the PnO. The effect of hcrt-1 (100 μM) on ACh release is shown in Fig. 5. Chromatographic peaks representing ACh in one

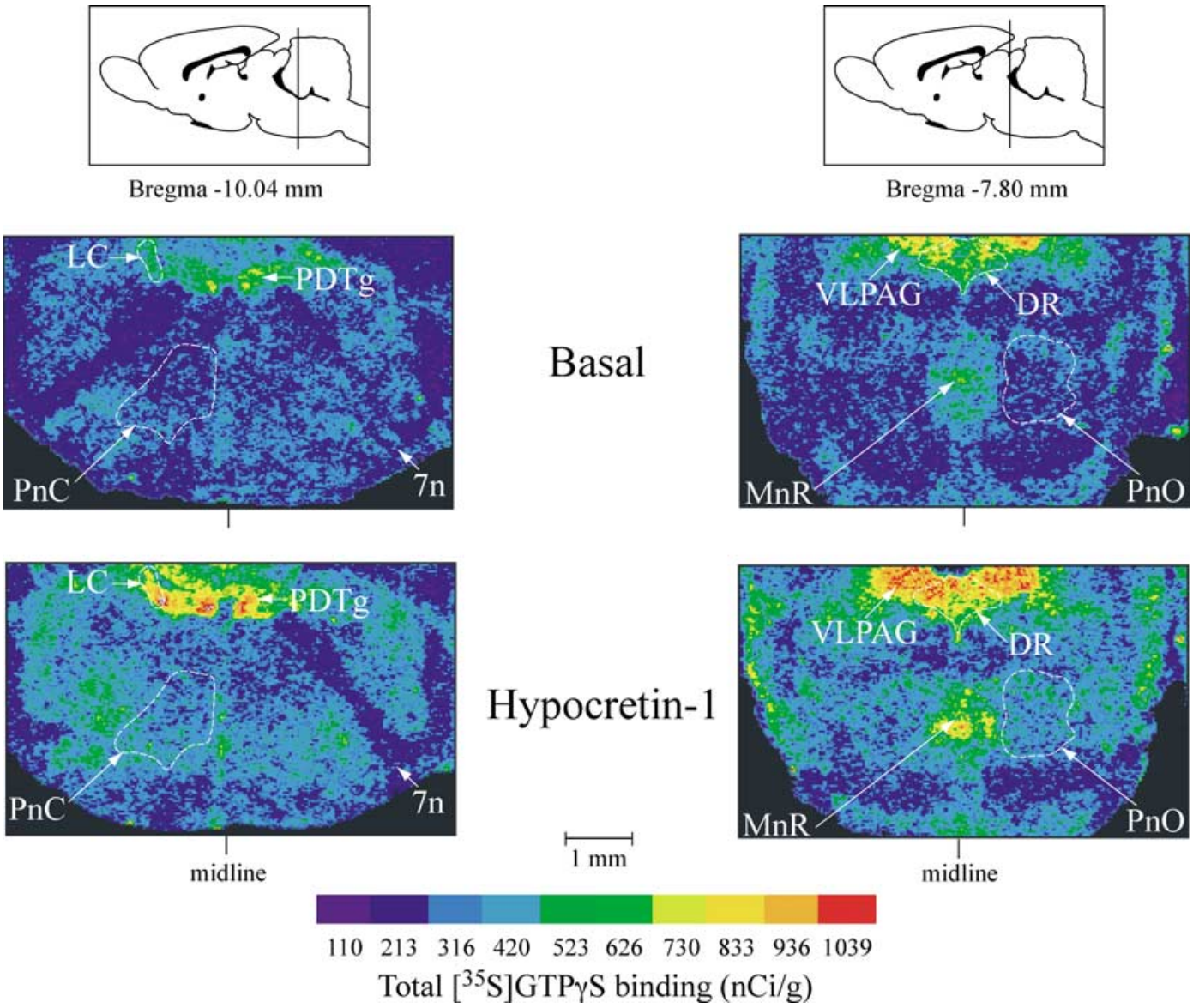

FIG. 1. Hcrt-1 activated G proteins in the pontine brain stem. Boxes at the top of each column show a sagittal schematic of the rat brain (from Paxinos & Watson, 1998). The vertical line in each schematic indicates the anterior–posterior level (relative to bregma) of the coronal autoradiograms shown below. The colour-coded autoradiograms illustrate total [^{35}S]GTPγS binding under basal conditions and following hcrt-1 (2000 nM) treatment.

sample obtained during dialysis with Ringer's (control) and one sample collected during dialysis delivery of hcrt-1 are presented in Fig. 5A. Figure 5B illustrates the time course of ACh release during one typical experiment. Each bar represents sequential ACh samples collected for 15 min. By the second sampling interval during dialysis delivery of hcrt-1, ACh release was clearly increased over control levels. Figure 5C summarizes data from six microdialysis experiments. Hcrt-1 significantly increased ACh release by an average of 87% ($t_5 = 5.6$, $P < 0.002$). Hcrt-1 had no significant effect on respiratory rate or core body temperature.

Discussion

The data reported here show that hcrt-1-induced [^{35}S]GTPγS binding in DR, LC and pontine reticular formation is concentration-dependent and blocked by a selective hcrt receptor antagonist. This is the first demonstration that, in brain stem nuclei known to regulate states of arousal, hcrt-1 activates G proteins as a consequence of specific receptor interactions. These results indicate that some hcrt receptors in the brain stem may couple to inhibitory (Gi-like) G proteins. This study also showed that *in vivo* administration of hcrt-1 to the pontine reticular formation increased ACh release in the pontine reticular formation. This finding suggests that hcrt may promote arousal by, in part, enhancing pontine cholinergic neurotransmission. The following discussion considers some of the strengths and limitations of the data, implications of the findings for G protein coupling of hcrt receptors, and inferences for arousal state control.

Hcrt-1-stimulated G protein activation is receptor-mediated

One advantage of *in vitro* [^{35}S]GTPγS autoradiography is that brain anatomy is preserved. Consequently, agonist-stimulated G protein activation can be quantified in specific histologically defined brain regions (Fig. 1). The present data show that for DR, LC, PnO and PnC, hcrt-1 caused a significant increase in [^{35}S]GTPγS binding which was

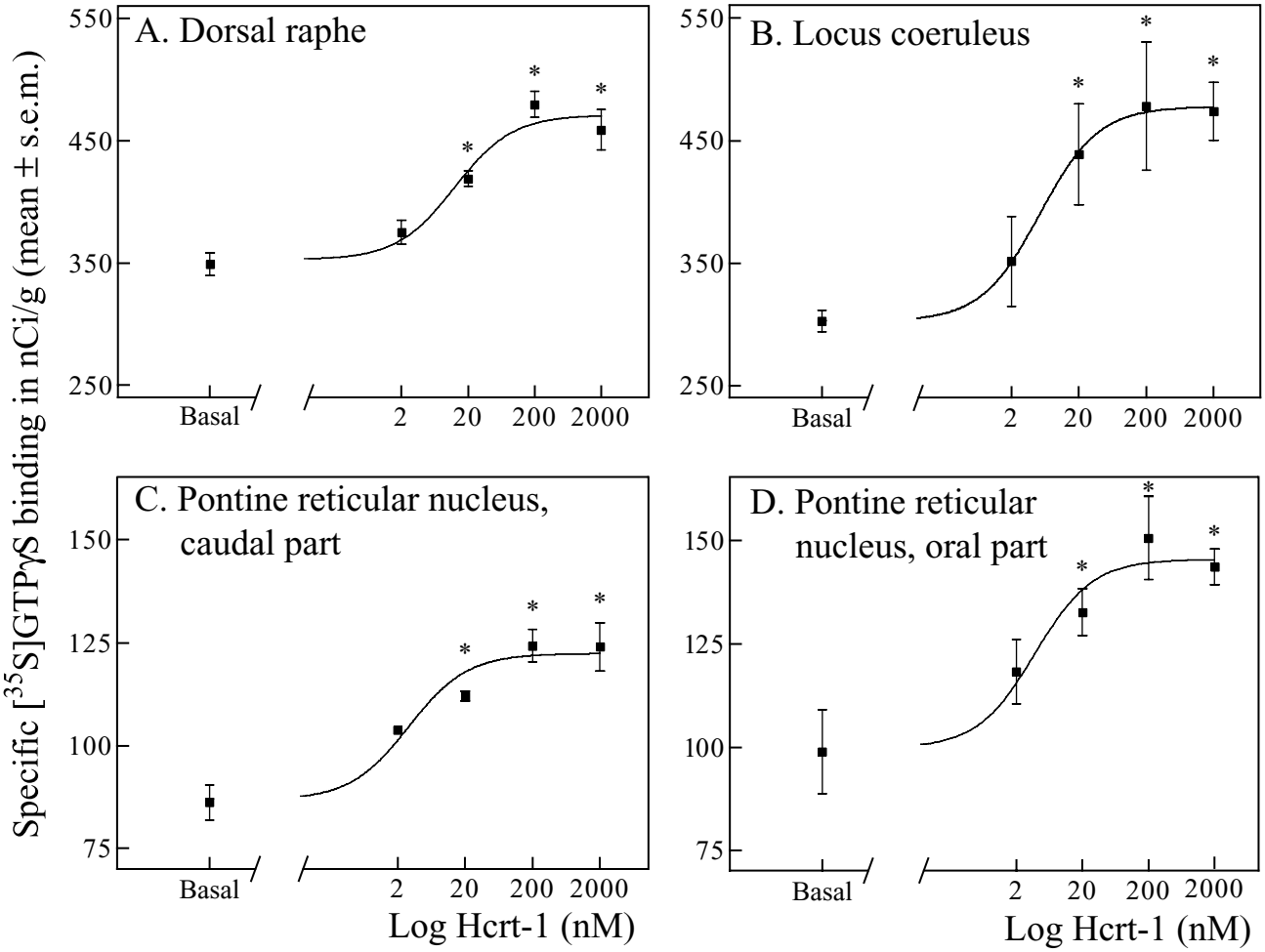

FIG. 2. Concentration-dependent G protein activation by hcrt-1 in (A) DR, (B) LC, (C) PnC and (D) PnO. Results were obtained from the following number (n) of individual measurements: DR, $n = 139$; LC, $n = 103$; PnC, $n = 299$; and PnO, $n = 203$. Specific [^{35}S]GTPγS binding following *in vitro* treatment with 20, 200, and 2000 nM hcrt-1 was significantly increased ($^*P < 0.05$) over basal G protein binding levels. A sigmoid concentration–response curve was fitted to the [^{35}S]GTPγS binding data for each nucleus. The resulting coefficients of determination (r^2) were 0.83 (DR), 0.56 (LC), 0.79 (PnC) and 0.69 (PnO). Thus, depending on brain region, 56–83% of the variance in [^{35}S]GTPγS binding was accounted for by the concentration of hcrt-1. The EC_{50} values (nM) calculated from these concentration–response data were 12.6 (DR), 5.3 (LC), 2.9 (PnC) and 3.8 (PnO). This finding indicates that hcrt-1 was less potent in DR than in the other nuclei studied.

concentration-dependent, reached saturation, and was fitted by a sigmoid curve (Fig. 2). Any biological process downstream from receptor binding which follows the law of mass action will exhibit a sigmoid shape when plotted as a semilogarithmic concentration–response curve (Taylor & Insel, 1990). This study therefore provides the first direct evidence that hcrt-1-stimulated [^{35}S]GTPγS binding in DR, LC, PnO and PnC is receptor-mediated.

Confirmation of a receptor-mediated response also is obtained by demonstrating pharmacological antagonism of the response (Limbird, 1996). This study used the competitive antagonist SB-334867 (Smart *et al*., 2001) to demonstrate that hcrt-1-induced G protein activation is receptor-mediated. SB-334867 has been shown to block electrophysiological (Soffin *et al*., 2002) and behavioural (Rodgers *et al*., 2001) responses to hcrt. Treatment of tissue sections with hcrt-1 plus SB-334867 reduced [^{35}S]GTPγS binding to basal levels in all four brain stem nuclei (Fig. 3), providing the first autoradiographic demonstration that hcrt-1-stimulated G protein activation can be pharmacologically antagonized. The present finding of antagonist blocking agrees with data showing that another hcrt receptor antagonist, NBI 36487, blocked hcrt-stimulated [^{35}S]GTPγS binding in homogenates of rat pons (Shiba *et al*., 2002). SB-334867 alone had no effect on [^{35}S]GTPγS binding (Fig. 3), consistent with reports that SB-334867 has no agonist activity (Smart *et al*., 2001).

Hcrt-1 activated G proteins in additional brain stem nuclei

G proteins were activated by hcrt-1 in regions medial to the LC, including the PDTg (Fig. 1). Some authors consider the PDTg of rat to be a homologue of the human dorsal tegmental nucleus, which relays autonomic impulses from the hypothalamus to the reticular formation (Huang *et al*., 1992). Hcrt-positive fibres have been reported in the intermediolateral cell column of the spinal cord in association with preganglionic sympathetic fibres (Date *et al*., 2000). Activation of PDTg also is consistent with functional studies indicating that hcrt excites sympathetic neurons (Antunes *et al*., 2001).

More rostrally in the brain stem, hcrt-1 activated regions near but outside the boundaries of the DR, including the VLPAG (Fig. 1). VLPAG plays a key role in nociceptive processing (Klamt & Prado, 1990). G proteins in VLPAG of mouse and rat are activated by the cholinergic agonist carbachol (DeMarco *et al*., 2003), and cholinergic antinociception has been demonstrated in rat (Ishizawa *et al*., 2000). The present observation that hcrt-1 activated G proteins in VLPAG of

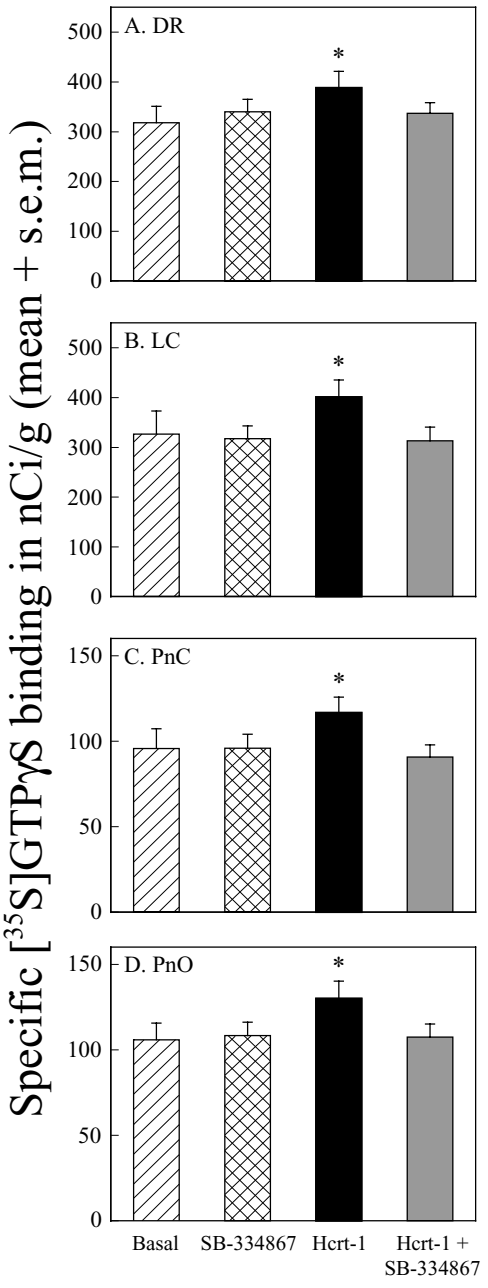

FIG. 3. Hcrt-1-stimulated [^{35}S]GTPγS binding was blocked by the hcrt receptor antagonist SB-334867. Results are based on the following number (n) of individual measurements: DR, $n = 295$; LC, $n = 158$; PnC, $n = 507$; and PnO, $n = 536$. The abscissa indicates the *in vitro* treatment condition: basal binding (no agonist or antagonist), SB-334867 (2 μM), hcrt-1 (200 nM), or hcrt-1 (200 nM) + SB-334867 (2 μM). $^{*}P < 0.05$ vs. basal [^{35}S]GTPγS binding.

rat is consistent with recent evidence that hcrt-1 can have antinociceptive effects (Yamamoto *et al*., 2002).

Finally, Fig. 1 shows that hcrt-1 activated G proteins in the MnR. Hcrt is a hypothalamic neuropeptide and hcrt-1 activation of G proteins in MnR is consistent with neuroanatomical data showing that MnR is the primary target of lateral hypothalamic fibres projecting to the brain stem (Vertes *et al*., 1999). Functional studies indicate that MnR activates hippocampus by mechanisms which include $GABA_A$- (Kinney *et al*., 1995) and $GABA_B$ (Varga *et al*., 2002)-mediated inhibition of serotonin-containing neurons.

It has been postulated that hcrt contributes to the regulation of arousal states, feeding and sensory–motor processing (Sakurai *et al*., 1998; Hagan *et al*., 1999; Yamamoto *et al*., 2002). Because these diverse functions involve regulation by a plethora of brain stem nuclei, it was anticipated that hcrt-1 would cause widespread activation of G proteins. The presently reported hcrt-stimulated G protein activation in multiple brain stem nuclei is consistent with the extensive regional distribution pattern of hcrt terminals (Peyron *et al*., 1998), receptor mRNA (Trivedi *et al*., 1998; Greco & Shiromani, 2001; Marcus *et al*., 2001) and receptor protein (Greco & Shiromani, 2001).

Two controls facilitate functional interpretation of the [^{35}S]GTPγS data. First, the cholinergic agonist carbachol was used as a positive control to confirm assay conditions, because carbachol has previously been shown to activate G proteins in pontine brain stem of rat (Capece *et al*., 1998) and mouse (DeMarco *et al*., 2003). In the present study, carbachol increased [^{35}S]GTPγS binding over basal levels in DR, LC, PnC and PnO by 77, 72, 94 and 74%, respectively, indicating that the assay was successful. Second, the *in vitro* autoradiography experiments included a brain region control. Figure 1 clearly shows lack of activation in the fibre pathway comprised of the facial nerve (7n).

Hcrt receptors and G protein subtypes

Hcrt-r1 and hcrt-r2 both signal through heterotrimeric G proteins (Sakurai *et al*., 1998). G proteins are classified into subtypes based on the selective interaction of the alpha subunit with a downstream signalling effector molecule (Farfel *et al*., 1999). The G protein subtypes coupled to hcrt receptors are still under investigation (reviewed in Kukkonen *et al*., 2002). Studies using hypothalamic neuronal cell cultures provided evidence that hcrt receptors increase intracellular calcium by coupling to Gq-like G proteins (van den Pol *et al*., 1998). Hcrt receptors have also been shown to cause direct activation of a calcium influx pathway (Lund *et al*., 2000). Recent *in vitro* work using rat (Nanmoku *et al*., 2000) or human (Karteris *et al*., 2001; Mazzocchi *et al*., 2001; Randeva *et al*., 2001) peripheral tissue suggests that hcrt receptors interact with Gi-like G proteins.

Agonist-activated [^{35}S]GTPγS binding is thought to preferentially label inhibitory G proteins (Kurkinen *et al*., 1997; Waeber & Moskowitz, 1997; Laitinen *et al*., 2001). Accordingly, the present finding that hcrt-1 causes a concentration-dependent antagonist-sensitive increase in [^{35}S]GTPγS binding may indicate that some hcrt receptors in rat brain stem couple to Gi-like G proteins. Several lines of evidence support this possibility. First, hcrt-induced stimulation of [^{35}S]GTPγS binding has also been demonstrated using Chinese hamster ovary cells expressing human hcrt-r2 and using homogenates of rat pons and midbrain (Shiba *et al*., 2002). Second, recent electrophysiological studies in human embryonic kidney (HEK) cell lines transfected with hcrt-r1 and hcrt-r2 revealed that pertussis toxin (PTX) blocked the hcrt-1-induced conductance increase (Hoang *et al*., 2003). Because PTX blocks inhibitory G proteins, this finding suggests that hcrt-r1 and hcrt-r2 can couple to multiple G protein subtypes, including Gi-like G proteins (Hoang *et al*., 2003). Third, *in vitro* studies in rat sympathetic preganglionic neurons showed that PTX pretreatment abolished hcrt-1-induced depolarization (van den Top *et al*., 2003). Fourth, preliminary autoradiographic data indicate that hcrt-1-stimulated [^{35}S]GTPγS binding in rat PnO is blocked by PTX (Bernard *et al*., 2003b). Fifth, in addition to its excitatory properties, hcrt-1 has been shown to simultaneously produce synaptic excitation and inhibition in the same set of neurons (Davis *et al*., 2003). These complexities illustrate that signalling pathways activated by hcrt-1 may differ in LC, DR and pontine reticular formation, despite involvement of the same G protein subtype. An alternate hypothesis is that hcrt-induced increases in [^{35}S]GTPγS binding are caused by indirect activation

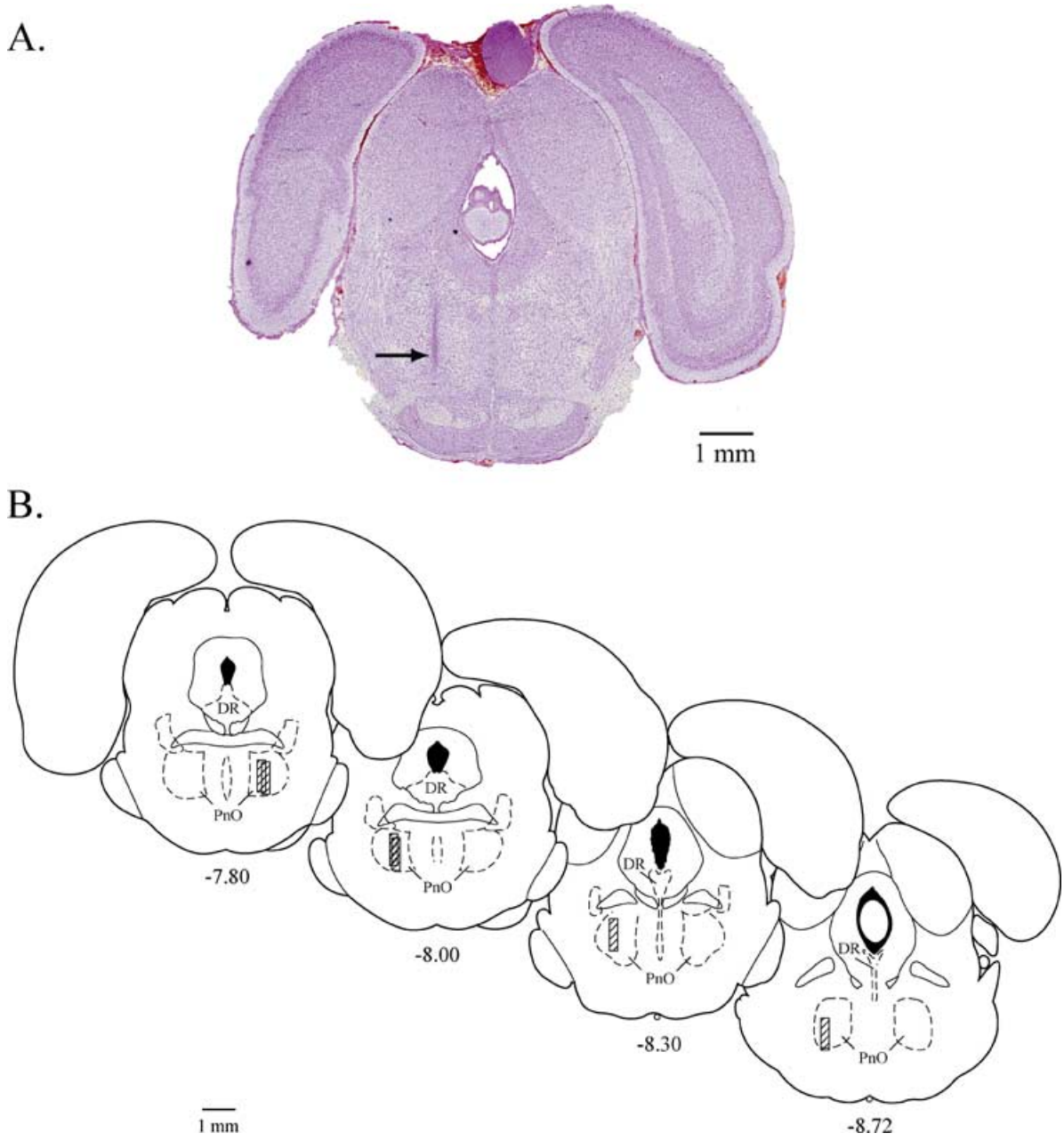

FIG. 4. Histological localization of dialysis sites. (A) Digitized image of a Cresyl Violet-stained brain stem section containing a lesion in the PnO made by a microdialysis probe (arrow). This section is located ≈7.9 mm posterior to bregma. Sections similar to this one were used for histological localization of microdialysis probes in all six animals. (B) Coronal rat brain atlas plates (Paxinos & Watson, 1998) from 7.80 to 8.72 mm posterior to bregma show the outlines and location of selected brain stem nuclei, including PnO. Hatched cylinders are drawn to scale and indicate the location of six dialysis sites within the PnO.

of Gi-like G proteins. Indirect activation could result from heterodimerization of hcrt receptors with other G protein-coupled receptors known to activate inhibitory G proteins (Devi, 2001; Angers *et al*., 2002; Brady & Limbird, 2002).

ACh release in PnO was modulated by hcrt-1

Having demonstrated that activation of hcrt receptors stimulates G proteins in arousal-related brain stem nuclei, this study next investigated the effect of hcrt-1 on ACh release. Direct administration of hcrt into the pontine brain stem increases either wakefulness or REM sleep, depending upon the nucleus injected. Microinjection of hcrt-1 into rat LC (Bourgin *et al*., 2000) or cat laterodorsal tegmental nucleus (LDT) (Xi *et al*., 2001) increases wakefulness and suppresses REM sleep. Microinjection of hcrt-1 into a terminal field of cholinergic LDT neurons, the pontine reticular formation, enhances REM sleep in cat (Xi *et al*., 2002). Hcrt neurons project to LDT (Peyron *et al*., 1998; Chemelli *et al*., 1999), and hcrt excites cholinergic LDT neurons (Burlet *et al*., 2002). Stimulating LDT and pedunculopontine tegmental nucleus (PPT) neurons causes cortical activation (Steriade, 1993) and increases ACh release in the pontine reticular formation (Lydic & Baghdoyan, 1993). The cortical activation of wakefulness and REM sleep (Moruzzi, 1972; Steriade, 1993) may be facilitated by excitatory hcrt input to these cholinergic brain stem neurons (Kilduff & Peyron, 2000).

Cortical ACh release reaches its greatest levels during wakefulness and REM sleep (Jasper & Tessier, 1971; Marrosu *et al*., 1995). In the

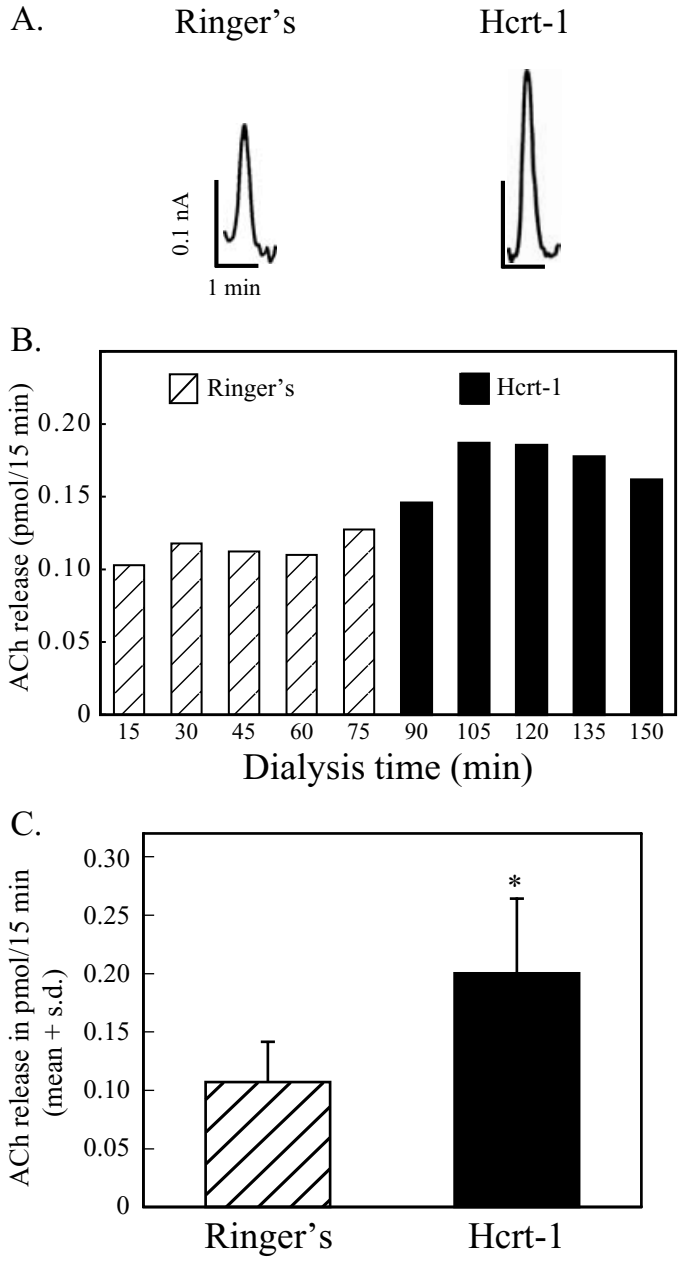

FIG. 5. Dialysis delivery of hcrt-1 into the PnO increased ACh release. (A) Two typical chromatograms from PnO dialysis samples obtained during administration of Ringer's (0.11 pmol ACh) or Ringer's containing hcrt-1 (0.19 pmol ACh). (B) Time course of ACh release from one representative microdialysis experiment. Hatched bars indicate ACh content in 30-μL samples collected during Ringer's (control) dialysis. Solid bars represent ACh release during dialysis with hcrt-1. (C) Data were averaged across time for control (Ringer's) samples and for hcrt-1 samples for each experiment, and then across experiments ($n = 6$) to show that hcrt-1 caused a significant ($^{*}P < 0.002$) increase in ACh release.

dorsal tegmental field rostral to LC (Kodama *et al*., 1990) and in the medial pontine reticular formation (Leonard & Lydic, 1997), ACh release is significantly greater during REM sleep than during wakefulness. ACh release in the medial pontine reticular formation also changes during the transition from halothane anaesthesia to postanaesthesia wakefulness (Keifer *et al*., 1996). ACh levels are low during anaesthesia and increase significantly during postanaesthesia wakefulness (Keifer *et al*., 1996). Taken together, the findings that (i) pontine reticular formation ACh release is increased during states characterized by cortical arousal (Keifer *et al*., 1996; Leonard & Lydic, 1997), (ii) hcrt promotes arousal (Kilduff & Peyron, 2000) and (iii) hcrt activates G proteins in the pontine reticular formation (present data) suggested the present hypothesis that hcrt-1 increases ACh release in the pontine reticular formation.

Dialysis administration of hcrt-1 to the PnO caused a significant increase in ACh release within the PnO (Figs 4 and 5). This is the first demonstration that hcrt-1 modulates the release of endogenous ACh *in vivo*. The results are compatible with the interpretation that one mechanism by which hcrt promotes arousal is by enhancing cholinergic transmission (Kilduff & Peyron, 2000). The present study did not include any dependent measures of arousal. Future experiments are needed to determine whether hcrt-induced ACh release in the pontine reticular formation is accompanied by cortical and/or behavioural activation. The present finding of increased ACh release caused by hcrt-1 is consistent with *in vitro* data showing that hcrt-1 increased [^{3}H]ACh outflow from enteric cholinergic nerve terminals in ileal strips (Matsuo *et al*., 2002).

Limitations, methodological considerations and conclusions

The effects of hcrt-1 on ACh release in PnC were not examined in the present study. PnC and PnO comprise the rat pontine reticular formation. The PnO was selected for dialysis because functional mapping studies of rat PnO and PnC have shown that the cholinergically evoked REM sleep-like state can be triggered with the shortest latency and greatest duration only from the caudal part of the PnO (Bourgin *et al*., 1995). This functional site-specificity stands in contrast to the finding that M2 muscarinic receptors are expressed throughout the pontine reticular formation with no difference in M2 receptor density between PnO and PnC (Baghdoyan, 1997). Previous [^{35}S]GTPγS studies also showed no difference in the magnitude of carbachol-stimulated G protein activation between PnO and PnC (Capece *et al*., 1998).

The present ACh release data were obtained using isoflurane-anaesthetized rat. Because ACh release in the medial (Leonard & Lydic, 1997) and dorsal tegmental (Kodama *et al*., 1990) portions of the pontine reticular formation changes significantly across the sleep-wake cycle, it was necessary to hold arousal state constant with general anaesthesia in order to distinguish between the effects of hcrt-1 and the effects of arousal state on ACh release. This approach has been used successfully to distinguish between drug- and state-induced changes in ACh release in cat pontine reticular formation (Baghdoyan *et al*., 1998) and basal forebrain (Vazquez & Baghdoyan, 2003), rat cortex (Materi *et al*., 2000) and mouse cortex (Douglas *et al*., 2001).

The relatively high concentration of hcrt-1 used for the present microdialysis experiments (100 μM) was selected based on *in vitro* data demonstrating that <0.1% of a peptide similar in molecular weight to hcrt is delivered through dialysis membranes (Kendrick, 1991). Thus, the estimated concentration of hcrt-1 delivered to the PnO was ≈100 nM. Hcrt-1-induced G protein activation in PnO occurred at concentrations ranging from 20 to 2000 nM (Fig. 2D). Future studies can determine whether the hcrt-1-induced increase in ACh release is concentration-dependent.

Limitations of the microdialysis technique preclude the ability to specify the mechanisms by which hcrt-1 significantly increased ACh release in PnO. Existing data regarding synaptic relationships and neurochemical identity of cells in the dorsolateral pons do, however, permit mechanistic speculation. Hcrt neurons are known to project to the pontine reticular formation (Peyron *et al*., 1998; Chemelli *et al*., 1999), and the pontine reticular formation has been shown to contain hcrt receptors (Greco & Shiromani, 2001; Hervieu *et al*., 2001). It is also known that rat PnO contains muscarinic cholinergic receptors

(Baghdoyan, 1997) and that PnO neurons are not cholinergic (Jones, 1990). The pontine reticular formation receives cholinergic input from the LDT/PPT (Mitani *et al*., 1988; Shiromani *et al*., 1988; Woolf & Butcher, 1989; Jones, 1990; Semba, 1993), and LDT/PPT neurons release ACh in the pontine reticular formation (Lydic & Baghdoyan, 1993). Thus, although the synaptic details remain unknown, it is clear that the hcrt-1-stimulated increase in ACh release must involve an effect on LDT/PPT cell bodies, LDT/PPT terminals in the PnO, or both.

How might hcrt-1 delivered to the PnO alter LDT/PPT terminals and/or cell bodies? Two possible mechanisms are considered here. First, hcrt-1 may facilitate ACh release by acting directly at hcrt receptors located presynaptically on cholinergic LDT/PPT terminals within PnO. Second, hcrt-1 depolarizes and increases the discharge rate of pontine reticular formation neurons *in vivo* (Xi *et al*., 2002). Pontine reticular formation neurons project to the LDT/PPT nuclei (Semba & Fibiger, 1992) and are thought to be glutamatergic (Kaneko *et al*., 1989; Stevens *et al*., 1992). Glutamate has been shown to excite cholinergic LDT/PPT neurons (Sanchez & Leonard, 1994). Thus, hcrt delivered by dialysis to the PnO may depolarize PnO neurons which in turn would depolarize LDT/PPT neurons, causing an increase in ACh release from LDT/PPT terminals in the PnO. The ability of PnO to alter LDT/PPT is supported by the finding that unilateral microinjection of carbachol into the pontine reticular formation causes increased ACh release in the contralateral pontine reticular formation (Lydic *et al*., 1991). The foregoing possible mechanisms are not mutually exclusive and hcrt-1 may modulate ACh release in PnO by a combination of these synaptic relationships. Although speculative, these possibilities are based on existing data and point the way for future experiments aiming to specify synaptic mechanisms by which hcrt-1 modulates ACh release.

The present finding that hcrt-1 increases ACh release in the PnO is novel and directly relevant to functional studies showing that hcrt-1 administration to PnO triggers a REM-sleep-like state (Xi *et al*., 2002). Whether hcrt-1 increases ACh release by activating an inhibitory G protein-coupled signal transduction pathway remains to be identified. The present results encourage future studies aiming to determine the synaptic location of hcrt receptors within the PnO.

Acknowledgements

This work was supported by NIH grants MH45361, HL57120, HL40881 and HL65272, and by the Department of Anaesthesiology. We thank GlaxoSmithKline for supplying SB-334867. G.N. Bowman, C.A. Lapham and M.A. Norat provided expert assistance.

Abbreviations

[^{35}S]GTPγS, [^{35}S]guanylyl-5′-O-(γ-thio)triphosphate; ACh, acetylcholine; DR, dorsal raphe nucleus; G protein, guanine nucleotide binding protein; GDP, guanosine 5′-diphosphate; GTPγS, guanosine 5′-O-(γ-thio)triphosphate; hcrt, hypocretin; hcrt-r, hypocretin receptor; LC, locus coeruleus; LDT, laterodorsal tegmental nucleus; MnR, median raphe nucleus; PDTg, posterodorsal tegmental nucleus; PnC, pontine reticular formation, caudal part; PnO, pontine reticular formation, oral part; PPT, pedunculopontine tegmental nucleus; PTX, pertussis toxin; REM, rapid eye movement; VLPAG, ventrolateral periaqueductal grey.

References

Angers, S., Salahpour, A. & Bouvier, M. (2002) Dimerization: an emerging concept for G protein-coupled receptor ontogeny and function. *Annu. Rev. Pharmacol. Toxicol.*, **42**, 409–435.

Antunes, V.R., Brailoiu, G.C., Kwok, E.H., Scruggs, P. & Dun, N.J. (2001) Orexins/hypocretins excite rat sympathetic preganglionic neurons in vivo and in vitro. *Am. J. Physiol. Regul. Integr. Comp. Physiol.*, **281**, R1801–R1807.

Baghdoyan, H.A. (1997) Location and quantification of muscarinic receptor subtypes in rat pons: implications for REM sleep generation. *Am. J. Physiol.*, **273**, R896–R904.

Baghdoyan, H.A., Lydic, R. & Fleegal, M.A. (1998) M2 muscarinic autoreceptors modulate acetylcholine release in the medial pontine reticular formation. *J. Pharmacol. Exp. Ther.*, **286**, 1446–1452.

Bernard, R., Lydic, R. & Baghdoyan, H.A. (2002a) Hypocretin-1 activates G proteins in arousal-related brainstem nuclei of rat. *Neuroreport*, **13**, 447–450.

Bernard, R., Lydic, R. & Baghdoyan, H.A. (2002b) The hypocretin receptor antagonist SB-334867 blocks hypocretin-1-induced G protein activation in sleep-related nuclei of rat brain stem. *Soc. Neurosci. Abstr.*, **28**, 870.4.

Bernard, R., Lydic, R. & Baghdoyan, H.A. (2003a) Hypocretin-1 increases acetylcholine (ACh) release in rat pontine reticular nucleus, oral part (PnO). *FASEB J.*, **17**, 390.6.

Bernard, R., Lydic, R. & Baghdoyan, H.A. (2003b) Pertussis toxin (PTX) blocks hypocretin-1-stimulated G protein activation in rat pontine reticular nucleus, oral part (PnO). *Soc. Neurosci. Abstr.*, **29**, in press.

Bourgin, P., Escourrou, P., Gaultier, C. & Adrien, J. (1995) Induction of rapid eye movement sleep by carbachol infusion into the pontine reticular formation in the rat. *Neuroreport*, **6**, 532–536.

Bourgin, P., Huitron-Resendiz, S., Spier, A.D., Fabre, V., Morte, B., Criado, J.R., Sutcliffe, J.G., Henriksen, S.J. & de Lecea, L. (2000) Hypocretin-1 modulates rapid eye movement sleep through activation of locus coeruleus neurons. *J. Neurosci.*, **20**, 7760–7765.

Brady, A.E. & Limbird, L.E. (2002) G protein-coupled receptor interacting proteins: Emerging roles in localization and signal transduction. *Cell. Signal.*, **14**, 297–309.

Brown, R.E., Sergeeva, O., Eriksson, K.S. & Haas, H.L. (2001) Orexin A excites serotonergic neurons in the dorsal raphe nucleus of the rat. *Neuropharmacology*, **40**, 457–459.

Burlet, S., Tyler, C.J. & Leonard, C.S. (2002) Direct and indirect excitation of laterodorsal tegmental neurons by hypocretin/orexin peptides: implications for wakefulness and narcolepsy. *J. Neurosci.*, **22**, 2862–2872.

Capece, M.L., Baghdoyan, H.A. & Lydic, R. (1998) Carbachol stimulates [^{35}S]guanylyl 5′-(γ-thio) triphosphate binding in REM sleep-related brain stem nuclei of rat. *J. Neurosci.*, **18**, 3779–3785.

Chemelli, R.M., Willie, J.T., Sinton, C.M., Elmquist, J.K., Scammell, T., Lee, C., Richardson, J.A., Williams, S.C., Xiong, Y., Kisanuki, Y., Fitch, T.E., Nakazato, M., Hammer, R.E., Saper, C.B. & Yanagisawa, M. (1999) Narcolepsy in *orexin* knockout mice: molecular genetics of sleep regulation. *Cell*, **98**, 437–451.

Date, Y., Mondal, M.S., Matsukura, S. & Nakazato, M. (2000) Distribution of orexin-A and orexin-B (hypocretins) in the rat spinal cord. *Neurosci. Lett.*, **288**, 87–90.

Davis, S.F., Williams, K.W., Xu, W., Glatzer, N.R. & Smith, B.N. (2003) Selective enhancement of synaptic inhibition by hypocretin (orexin) in rat vagal motor neurons: implications for autonomic regulation. *J. Neurosci.*, **23**, 3844–3854.

DeMarco, G.J., Baghdoyan, H.A. & Lydic, R. (2003) Differential cholinergic activation of G proteins in rat and mouse brainstem: relevance for sleep and nociception. *J. Comp. Neurol.*, **457**, 175–184.

Devi, L.A. (2001) Heterodimerization of G-protein-coupled receptors: pharmacology, signaling and trafficking. *Trends Pharmacol. Sci.*, **22**, 532–537.

Douglas, C.L., Baghdoyan, H.A. & Lydic, R. (2001) M2 muscarinic autoreceptors modulate acetylcholine release in prefrontal cortex of C57BL/6J mouse. *J. Pharmacol. Exp. Ther.*, **229**, 960–966.

Duxon, M.S., Stretton, J., Starr, K., Jones, D.N.C., Holland, V., Riley, G., Jerman, J.C., Brough, S., Smart, D., Johns, A., Chan, W., Porter, R.A. & Upton, N. (2001) Evidence that orexin-A-evoked grooming in the rat is mediated by orexin-1 (OX_1) receptors, with downstream 5-HT_{2C} receptor involvement. *Psychopharmacology*, **153**, 203–209.

España, R.A., Baldo, B.A., Kelley, A.E. & Berridge, C.W. (2001) Wake-promoting and sleep-suppressing actions of hypocretin (orexin): basal forebrain sites of action. *Neuroscience*, **106**, 699–715.

Farfel, Z., Bourne, H.R. & Iiri, T. (1999) The expanding spectrum of G protein diseases. *New Engl. J. Med.*, **340**, 1012–1020.

Gerashchenko, D., Kohls, M.D., Greco, M., Waleh, N.S., Salin-Pascual, R., Kilduff, T.S., Lappi, D.A. & Shiromani, P.J. (2001) Hypocretin-2-saporin lesions of the lateral hypothalamus produce narcoleptic-like sleep behavior in the rat. *J. Neurosci.*, **21**, 7273–7283.

Greco, M.A. & Shiromani, P.J. (2001) Hypocretin receptor protein and mRNA expression in the dorsolateral pons of rats. *Brain Res. Mol. Brain Res.*, **88**, 176–182.

Hagan, J.J., Leslie, R.A., Patel, S., Evans, M.L., Wattam, T.A., Holmes, S., Benham, C.D., Taylor, S.G., Routledge, C., Hemmati, P., Munton, R.P.,

Ashmeade, T.E., Shah, A.S., Hatcher, J.P., Hatcher, P.D., Jones, D.N., Smith, M.I., Piper, D.C., Hunter, A.J., Porter, R.A. & Upton, N. (1999) Orexin A activates locus coeruleus cell firing and increases arousal in the rat. *Proc. Natl Acad. Sci. USA*, **96**, 10911–10916.

Hara, J., Beuckmann, C.T., Nambu, T., Willie, J.T., Chemelli, R.M., Sinton, C.M., Sugiyama, F., Yagami, K., Goto, K., Yanagisawa, M. & Sakurai, T. (2001) Genetic ablation of orexin neurons in mice results in narcolepsy, hypophasia, and obesity. *Neuron*, **30**, 345–354.

Hervieu, G.J., Cluderay, J.E., Harrison, D.C., Roberts, J.C. & Leslie, R.A. (2001) Gene expression and protein distribution of the orexin-1 receptor in the rat brain and spinal cord. *Neuroscience*, **103**, 777–797.

Hoang, Q.V., Bajic, D., Yanagisawa, M., Nakajima, S. & Nakajima, Y. (2003) Effects of orexin (hypocretin) on GIRK channels. *J. Neurophysiol.*, **90**, 695–702.

Horvath, T.L., Peyron, C., Diano, S., Ivanov, A., Aston-Jones, G., Kilduff, T.S. & van Den Pol, A.N. (1999) Hypocretin (orexin) activation and synaptic innervation of the locus coeruleus noradrenergic system. *J. Comp. Neurol.*, **415**, 145–159.

Huang, X.-F., Törk, I., Halliday, G.M. & Paxinos, G. (1992) The dorsal, posterodorsal, and ventral tegmental nuclei: a cyto- and chemoarchitectonic study in the human. *J. Comp. Neurol.*, **318**, 117–137.

Ishizawa, Y., Ma, H.-C., Dohi, S. & Shimonaka, H. (2000) Effects of cholinomimetic injection into the brain stem reticular formation on halothane anesthesia and antinociception in rats. *J. Pharmacol. Exp. Ther.*, **293**, 845–851.

Jasper, H.H. & Tessier, J. (1971) Acetylcholine liberation from cerebral cortex during paradoxical (REM) sleep. *Science*, **172**, 601–602.

Jones, B.E. (1990) Immunohistochemical study of choline acetyltransferase-immunoreactive processes and cells innervating the pontomedullary reticular formation in the rat. *J. Comp. Neurol.*, **295**, 485–514.

Kaneko, T., Itoh, K., Shigemoto, R. & Mizuno, N. (1989) Glutamine-like immunoreactivity in the lower brainstem and the cerebellum of the adult rat. *Neuroscience*, **32**, 79–98.

Karteris, E., Randeva, H.S., Grammatopoulos, D.K., Jaffe, R.B. & Hillhouse, E.W. (2001) Expression and coupling characteristics of the CRH and orexin type 2 receptors in human fetal adrenals. *J. Clin. Endocrinol. Metab.*, **86**, 4512–4519.

Keifer, J.C., Baghdoyan, H.A. & Lydic, R. (1996) Pontine cholinergic mechanisms modulate the cortical EEG spindles of halothane anesthesia. *Anesthesiology*, **84**, 945–954.

Kendrick, K.M. (1991) *In Vitro Recovery Measurements of Peptides*. Peptide Measurement Product Catalog. CMA/Microdialysis, Stockholm, Sweden.

Kilduff, T.S. & Peyron, C. (2000) The hypocretin/orexin ligand-receptor system: implications for sleep and sleep disorders. *Trends Neurosci.*, **23**, 359–365.

Kinney, G.G., Kocsis, B. & Vertes, R.P. (1995) Injections of muscimol into the median raphe nucleus produce hippocampal theta rhythm in the urethane anesthetized rat. *Psychopharmacology*, **120**, 244–248.

Klamt, J.G. & Prado, W.A. (1990) Antinociception and behavioral changes induced by carbachol microinjected into identified sites of the rat brain. *Brain Res.*, **549**, 9–18.

Kodama, T., Takahashi, Y. & Honda, Y. (1990) Enhancement of acetylcholine release during paradoxical sleep in the dorsal tegmental field of the cat brain stem. *Neurosci. Lett.*, **114**, 277–282.

Kukkonen, J.P., Holmqvist, T., Ammoun, S. & Åkerman, K.E. (2002) Functions of the orexinergic/hypocretinergic system. *Am. J. Physiol. Cell. Physiol.*, **283**, C1567–C1591.

Kurkinen, K.M.A., Koistinaho, J. & Laitinen, J.T. (1997) [γ-^{35}S]GTP autoradiography allows region-specific detection of muscarinic receptor-dependent G-protein activation in chick optic tectum. *Brain Res.*, **769**, 21–28.

Laitinen, J.T., Asko, U., Raidaru, G. & Miettinen, R. (2001) [^{35}S]GTPγS autoradiography reveals a wide distribution of $G_{i/o}$-linked ADP receptors in the nervous system: close similarities with the platelet *P2Y$_{ADP}$* receptor. *J. Neurochem.*, **77**, 505–518.

de Lecea, L., Kilduff, T.S., Peyron, C., Gao, X., Foye, P.E., Danielson, P.E., Fukuhara, C., Battenberg, E.L., Gautvik, V.T., Bartlett, F.S., 2nd, Frankel, W.N., van den Pol, A.N., Bloom, F.E., Gautvik, K.M. & Sutcliffe, J.G. (1998) The hypocretins: hypothalamus-specific peptides with neuroexcitatory activity. *Proc. Natl Acad. Sci. USA*, **95**, 322–327.

Leonard, T.O. & Lydic, R. (1997) Pontine nitric oxide modulates acetylcholine release, rapid eye movement sleep generation, and respiratory rate. *J. Neurosci.*, **17**, 774–785.

Limbird, L.E. (1996) *Cell Surface Receptors: a Short Course on Theory and Methods*, 2nd edn. Martinus-Nijhoff Publishing, Boston.

Lin, L., Faraco, J., Li, R., Kadotani, H., Rogers, W., Lin, X., Qiu, X., de Jong, P.J., Nishino, S. & Mignot, E. (1999) The sleep disorder canine narcolepsy is caused by a mutation in the hypocretin (orexin) receptor 2 gene. *Cell*, **98**, 365–376.

Lund, P.-E., Shariatmadari, R., Uustare, A., Detheux, M., Parmentier, M., Kukkonen, J.P. & Åkerman, K.E.O. (2000) The orexin OX_1 receptor activates a novel Ca^{2+} influx pathway necessary for coupling to phospholipase C. *J. Biol. Chem.*, **275**, 30806–30812.

Lydic, R. & Baghdoyan, H.A. (1993) Pedunculopontine stimulation alters respiration and increases ACh release in the pontine reticular formation. *Am. J. Physiol.*, **264**, R544–R554.

Lydic, R., Baghdoyan, H.A. & Lorinc, Z. (1991) Microdialysis of cat pons reveals enhanced acetylcholine release during state-dependent respiratory depression. *Am. J. Physiol.*, **261**, R766–R770.

Marcus, J.N., Aschkenasi, C.J., Lee, C.E., Chemelli, R.M., Saper, C.B., Yanagisawa, M. & Elmquist, J.K. (2001) Differential expression of orexin receptors 1 and 2 in the rat brain. *J. Comp. Neurol.*, **435**, 6–25.

Marrosu, F., Portas, C., Mascia, M.S., Casu, M.A., Fa, M., Giagheddu, M., Imperato, A. & Gessa, G.L. (1995) Microdialysis measurement of cortical and hippocampal acetylcholine release during sleep–wake cycle in freely moving cats. *Brain Res.*, **671**, 329–332.

Materi, L.M., Rasmusson, D.D. & Semba, K. (2000) Inhibition of synaptically evoked cortical acetylcholine release by adenosine: an *in vivo* microdialysis study in the rat. *Neuroscience*, **97**, 219–226.

Matsuo, K., Kaibara, M., Uezono, Y., Hayashi, H., Taniyama, K. & Nakane, Y. (2002) Involvement of cholinergic neurons in orexin-induced contraction of guinea pig ileum. *Eur. J. Pharmacol.*, **452**, 105–109.

Mazzocchi, G., Malendowicz, L.K., Aragona, F., Rebuffat, P., Gottardo, L. & Nussdorfer, G.G. (2001) Human pheochromocytomas express orexin receptor type 2 gene and display an in vitro secretory response to orexins A and B. *J. Clin. Endocrinol. Metab.*, **86**, 4818–4821.

Mitani, A., Ito, K., Hallanger, A.E., Wainer, B.H., Kataoka, K. & McCarley, R.W. (1988) Cholinergic projections from the laterodorsal and pedunculopontine tegmental nuclei to the pontine gigantocellular tegmental field in the cat. *Brain Res.*, **451**, 397–402.

Moruzzi, G. (1972) The sleep–waking cycle. *Ergebn. Physiol.*, **64**, 1–165.

Nanmoku, T., Isobe, K., Sakurai, T., Yamanaka, A., Takekoshi, K., Kawakami, Y., Ishii, K., Goto, K. & Nakai, T. (2000) Orexins suppress catecholamine synthesis and secretion in cultured PC12 cells. *Biochem. Biophys. Res. Com.*, **274**, 310–315.

Nishino, S. & Mignot, E. (1997) Pharmacological aspects of human and canine narcolepsy. *Prog. Neurobiol.*, **52**, 27–78.

Nishino, S., Ripley, B., Overeem, S., Lammers, G.J. & Mignot, E. (2000) Hypocretin (orexin) deficiency in human narcolepsy. *Lancet*, **355**, 39–40.

Nishino, S., Ripley, B., Overeem, S., Nevsimalova, S., Lammers, G.J., Vankova, J., Okun, M., Rogers, W., Brooks, S. & Mignot, E. (2001) Low cerebrospinal fluid hypocretin (orexin) and altered energy homeostasis in human narcolepsy. *Ann. Neurol.*, **50**, 381–388.

Paxinos, G. & Watson, C. (1998) *The Rat Brain in Stereotaxic Coordinates*, 4th edn. Academic Press, New York.

Peyron, C., Faraco, J., Rogers, W., Ripley, B., Overeem, S., Charnay, Y., Nevsimalova, S., Aldrich, M., Reynolds, D., Albin, R., Li, R., Hungs, M., Pedrazzoli, M., Padigaru, M., Kucherlapati, M., Fan, J., Maki, R., Lammers, G.J., Bouras, C., Kucherlapati, R., Nishino, S. & Mignot, E. (2000) A mutation in a case of early onset narcolepsy and a generalized absence of hypocretin peptides in human narcoleptic brains. *Nature Med.*, **6**, 991–997.

Peyron, C., Tighe, D.K., van den Pol, A.N., de Lecea, L., Heller, H.C., Sutcliffe, J.G. & Kilduff, T.S. (1998) Neurons containing hypocretin (orexin) project to multiple neuronal systems. *J. Neurosci.*, **18**, 9996–10015.

Piper, D.C., Upton, N., Smith, M.I. & Hunter, A.J. (2000) The novel brain neuropeptide, orexin-A, modulates the sleep–wake cycle of rats. *Eur. J. Neurosci.*, **12**, 726–730.

van den Pol, A.N., Gao, X.B., Obrietan, K., Kilduff, T.S. & Belousov, A.B. (1998) Presynaptic and postsynaptic actions and modulation of neuroendocrine neurons by a new hypothalamic peptide, hypocretin/orexin. *J. Neurosci.*, **18**, 7962–7971.

Randeva, H.S., Karteris, E., Grammatopoulos, D. & Hillhouse, E.W. (2001) Expression of orexin-A and functional orexin type 2 receptors in the human adult adrenals: implications for adrenal function and energy homeostasis. *J. Clin. Endocrinol. Metab.*, **86**, 4808–4813.

Rodgers, R.J., Halford, J.C.G., Nunes de Souza, R.L., Canto de Souza, A.L., Piper, D.C., Arch., J.R.S., Upton, N., Porter, R.A., Johns, A. & Blundell, J.E. (2001) SB-334867, a selective orexin-1 receptor antagonist, enhances behavioral satiety and blocks the hyperphagic effect of orexin-A in rats. *Eur. J. Neurosci.*, **13**, 1444–1452.

Sakurai, T., Amemiya, A., Ishii, M., Matsuzaki, I., Chemelli, R.M., Tanaka, H., Williams, S.C., Richardson, J.A., Kozlowski, G.P., Wilson, S., Arch., J.R.,

Buckingham, R.E., Haynes, A.C., Carr, S.A., Annan, R.S., McNulty, D.E., Liu, W.S., Terrett, J.A., Elshourbagy, N.A., Bergsma, D.J. & Yanagisawa, M. (1998) Orexins and orexin receptors: a family of hypothalamic neuropeptides and G protein-coupled receptors that regulate feeding behavior. *Cell*, **92**, 573–585.

Sanchez, R. & Leonard, C.S. (1994) NMDA receptor-mediated synaptic input to nitric oxide synthase-containing neurons of the guinea pig mesopontine tegmentum in vitro. *Neurosci. Lett.*, **197**, 141–144.

Scammell, T.E. (2003) The neurobiology, diagnosis, and treatment of narcolepsy. *Ann. Neurol.*, **53**, 154–166.

Semba, K. (1993) Aminergic and cholinergic afferents to REM sleep induction regions of the pontine reticular formation in the rat. *J. Comp. Neurol.*, **330**, 543–556.

Semba, K. & Fibiger, H.C. (1992) Afferent connections of the laterodorsal and the pedunculopontine tegmental nuclei in rat: a retro- and antero-grade transport and immunohistochemical study. *J. Comp. Neurol.*, **323**, 387–410.

Shiba, T., Ozu, M., Yoshida, Y., Mignot, E. & Nishino, S. (2002) Hypocretin stimulates [^{35}S]GTPγS binding in hcrtr 2-transfected cell lines and in brain homogenate. *Biochem. Biophys. Res. Com.*, **294**, 615–620.

Shiromani, P.J., Armstrong, D.M. & Gillin, J.C. (1988) Cholinergic neurons from the dorsolateral pons project to the medial pons: a WGA-HRP and choline acetyltransferase immunohistochemical study. *Neurosci. Lett.*, **95**, 19–23.

Sim, L.J., Selley, D.E. & Childers, S.R. (1995) *In vitro* autoradiography of receptor-activated G proteins in rat brain by agonist-stimulated guanylyl 5′-[γ-[^{35}S]thio]-triphosphate binding. *Proc. Natl Acad. Sci. USA*, **92**, 7242–7246.

Smart, D., Sabido-David, C., Brough, S.J., Jewitt, F., Johns, A., Porter, R.A. & Jerman, J.C. (2001) SB-334867-A: the first selective orexin-1 receptor antagonist. *Br. J. Pharmacol.*, **132**, 1179–1182.

Soffin, E.M., Evans, M.L., Gill, C.H., Harries, M.H., Benham, C.D. & Davies, C.H. (2002) SB-334867-A antagonises orexin mediated excitation in the locus coeruleus. *J. Neuropharmacol.*, **42**, 127–133.

Sóvágó, J., Dupuis, D.S. & Gulyás, B. (2001) An overview on functional receptor autoradiography using [^{35}S]GTPγS autoradiography. *Brain Res. Rev.*, **38**, 148–164.

Steriade, M. (1993) Cholinergic blockage of network- and intrinsically-generated slow oscillations promotes waking and REM sleep activity patterns in thalamic and cortical neurons. *Prog. Brain Res.*, **98**, 345–355.

Stevens, D.R., McCarley, R.W. & Greene, R.W. (1992) Excitatory amino acid-mediated responses and synaptic potentials in medial pontine reticular formation neurons of the rat *in vitro*. *J. Neurosci.*, **12**, 4188–4194.

Taylor, P. & Insel, P.A. (1990) Molecular basis of pharmacologic selectivity. In Pratt, W.B. & Taylor, P. (eds), *Principles of Drug Action: the Basis of Pharmacology*. Churchill Livingstone, New York, pp. 1–102.

Thannickal, T.C., Moore, R.Y., Nienhuis, R., Ramanathan, L., Gulyani, S., Aldrich, M., Comford, M. & Siegel, J.M. (2000) Reduced number of hypocretin neurons in human narcolepsy. *Neuron*, **27**, 469–474.

van den Top, M., Nolan, M.F., Lee, K., Richardson, P.J., Buijs, R.M., Davies, C. & Spanswick, D. (2003) Orexins induce increased excitability and synchronisation of rat sympathetic preganglionic neurones. *J. Physiol. (Lond.)*, **549**, 809–821.

Trivedi, P., YuH., MacNeil, D.J., Van der Ploeg, L.H.T. & Guan, X.-M. (1998) Distribution of orexin receptor mRNA in the rat brain. *FEBS Lett.*, **438**, 71–75.

Varga, V., Sik, A., Freund, T.F. & Kocsis, B. (2002) $GABA_B$ receptors in the median raphe nucleus: Distribution and role in the serotonergic control of hippocampal activity. *Neuroscience*, **109**, 119–132.

Vazquez, J. & Baghdoyan, H.A. (2003) Muscarinic and $GABA_A$ receptors modulate acetylcholine release in feline basal forebrain. *Eur. J. Neurosci.*, **17**, 249–259.

Vertes, R.P., Fortin, W.J. & Crane, A.M. (1999) Projections of the median raphe nucleus in the rat. *J. Comp. Neurol.*, **407**, 555–582.

Waeber, C. & Moskowitz, M.A. (1997) 5-hydroxytryptamine$_{1A}$ and 5-hydroxytryptamine$_{1B}$ receptors stimulated [^{35}S]guanosine-5′-*O*-(3-thio) triphosphate binding to rodent brain sections as visualized by *in vitro* autoradiography. *Mol. Pharmacol.*, **52**, 623–631.

Woolf, N.J. & Butcher, L.L. (1989) Cholinergic systems in the rat brain. IV. Descending projections of the pontomesencephalic tegmentum. *Brain Res. Bull.*, **23**, 519–540.

Xi, M.-C., Fung, S.J., Yamuy, J., Morales, F.R. & Chase, M.H. (2002) Induction of active (REM) sleep by microinjection of hypocretin into the nucleus pontis oralis of the cat. *J. Neurophysiol.*, **87**, 2880–2888.

Xi, M., Morales, F.R. & Chase, M.H. (2001) Effects on sleep and wakefulness of the injection of hypocretin-1 (orexin-A) into the laterodorsal tegmental nucleus of the cat. *Brain Res.*, **901**, 259–264.

Yamamoto, T., Nozaki-Taguchi, N. & Chiba, T. (2002) Analgesic effect of intrathecally administered orexin-A in the rat formalin test and in the rat hot plate test. *Br. J. Pharmacol.*, **137**, 170–176.